Synthesis and Evaluation of 1,2,8,8a-Tetrahydrocyclopropa[*c*]pyrrolo[3,2-*e*]indol-4(5*H*)-one, the Parent Alkylation Subunit of CC-1065 and the Duocarmycins: Impact of the Alkylation Subunit Substituents and Its Implications for DNA Alkylation Catalysis

Dale L. Boger,* Alejandro Santillán, Jr., Mark Searcey, Steven R. Brunette, Scott E. Wolkenberg, Michael P. Hedrick, and Qing Jin

Department of Chemistry and The Skaggs Institute for Chemical Biology, The Scripps Research Institute, 10550 North Torrey Pines Road, La Jolla, California 92037

Received March 3, 2000

The synthesis of 1,2,8,8a-tetrahydrocyclopropa[*c*]pyrrolo[3,2-*e*]indol-4(5*H*)-one (CPI), the parent CC-1065 and duocarmycin SA alkylation subunit, is detailed. The parent CPI alkylation subunit lacks the C7 methyl substituent of the CC-1065 alkylation subunit and the C6 methoxycarbonyl group of duocarmycin SA, and their examination permitted the establishment of the impact of these natural product substituents. The studies revealed a CPI stability comparable to the CC-1065 alkylation subunit but which was 6× more reactive than the (+)-duocarmycin SA alkylation subunit, and it displayed the inherent reaction regioselectivity (4:1) of the natural products. The single-crystal X-ray structure of (+)-*N*-BOC-CPI depicts a near identical stereoelectronic alignment of the cyclopropane accounting for the identical reaction regioselectivity and a slightly diminished vinylogous amide conjugation relative to (+)-*N*-BOC-DSA suggesting that the stability distinctions stem in part from this difference in the vinylogous amide as well as alterations in the electronic nature of the fused pyrrole. Establishment of the DNA binding properties revealed that the CPI-based agents retain the identical DNA alkylation selectivities of the natural products. More importantly, the C6 methoxycarbonyl group of duocarmycin SA was found to increase the rate (12−13×) and efficiency (10×) of DNA alkylation despite its intrinsic lower reactivity while the CC-1065 C7 methyl group was found to slow the DNA alkylation rate (4×) and lower the alkylation efficiency (ca. 4×). The greater DNA alkylation rate and efficiency for duocarmycin SA and related analogues containing the C6 methoxycarbonyl is proposed to be derived from the extended length that the rigid C6 methoxycarbonyl provides and the resulting increase in the DNA binding-induced conformational change which serves to deconjugate the vinylogous amide and activate the alkylation subunit for nucleophilic attack. The diminished properties resulting from the CC-1065 C7 methyl group may be attributed to the steric impediment this substituent introduces to DNA minor groove binding and alkylation. Consistent with this behavior, the duocarmycin SA C6 methoxycarbonyl group increases biological potency while the CC-1065 C7 methyl group diminishes it.

Introduction. CC-1065 and the duocarmycins form the parent members of a class of potent antitumor antibiotics that selectively bind and alkylate DNA (Figure 1).[1] The stereoelectronically controlled adenine N3 addition to the least substituted carbon of the activated cyclopropane occurs within selected minor groove AT-rich sites, and extensive effort has been devoted to determine the origin of the DNA alkylation selectivity, to establish the link between DNA alkylation and the ensuing biological properties, and to define the fundamental principles underlying the relationships between structure, chemical reactivity, and biological activity.[2−5]

Key to recent studies was the identification of a conformational change induced upon binding in the narrow AT-rich minor groove, which leads to disruption of the vinylogous amide stabilization of the alkylation subunit and activation of the cyclopropane to nucleophilic attack.[6] This subtle element of the DNA alkylation mechanism was initially recognized through the synthe-

(1) Ichimura, M.; Ogawa, T.; Takahashi, K.; Kobayashi, E.; Kawamoto, I.; Yasuzawa, T.; Takahashi, I.; Nakano, H. *J. Antibiot.* **1990**, *43*, 1037. Ichimura, M.; Ogawa, T.; Katsumata, S.; Takahashi, K.; Takahashi, I.; Nakano, H. *J. Antibiot.* **1991**, *44*, 1045. Ohba, K.; Watabe, H.; Sasaki, T.; Takeuchi, Y.; Kodama, Y.; Nakazawa, T.; Yamamoto, H.; Shomura, T.; Sezaki, M.; Kondo, S. *J. Antibiot.* **1988**, *41*, 1515. Takahashi, I.; Takahashi, K.; Ichimura, M.; Morimoto, M.; Asano, K.; Kawamoto, I.; Tomita, F.; Nakano, H. *J. Antibiot.* **1988**, *41*, 1915. Yasuzawa, T.; Iida, T.; Muroi, K.; Ichimura, M.; Takahashi, K.; Sano, H. *Chem. Pharm. Bull.* **1988**, *36*, 3728. Ichimura, M.; Muroi, K.; Asano, K.; Kawamoto, I.; Tomita, F.; Morimoto, M.; Nakano, H. *J. Antibiot.* **1988**, *41*, 1285. Ishii, S.; Nagasawa, M.; Kariya, Y.; Yamamoto, H.; Inouye, S.; Kondo, S. *J. Antibiot.* **1989**, *42*, 1713. Hanka, L. J.; Dietz, A.; Gerpheide, S. A.; Kuentzel, S. L.; Martin, D. G. *J. Antibiot.* **1978**, *31*, 1211. Chidester, C. G.; Krueger, W. C.; Mizsak, S. A.; Duchamp, D. J.; Martin, D. G. *J. Am. Chem. Soc.* **1981**, *103*, 7629.

(2) Boger, D. L.; Machiya, K.; Hertzog, D. L.; Kitos, P. A.; Holmes, D. *J. Am. Chem. Soc.* **1993**, *115*, 9025.

(3) For mechanistic aspects see: Boger, D. L.; Johnson, D. S. *Angew. Chem., Int. Ed. Engl.* **1996**, *35*, 1438.

(4) For synthetic aspects see: Boger, D. L.; Boyce, C. W.; Garbaccio, R. M.; Goldberg, J. A. *Chem. Rev.* **1997**, *97*, 787.

(5) Warpehoski, M. A.; Hurley, L. H. *Chem. Res. Toxicol.* **1988**, *1*, 315.

(6) Boger, D. L.; Garbaccio, R. M. *Acc. Chem. Res.* **1999**, *32*, 1043. Boger, D. L.; Garbaccio, R. M. *Bioorg. Med. Chem.* **1997**, *5*, 263.

10.1021/jo000297j CCC: $19.00
Published on Web 05/10/2000

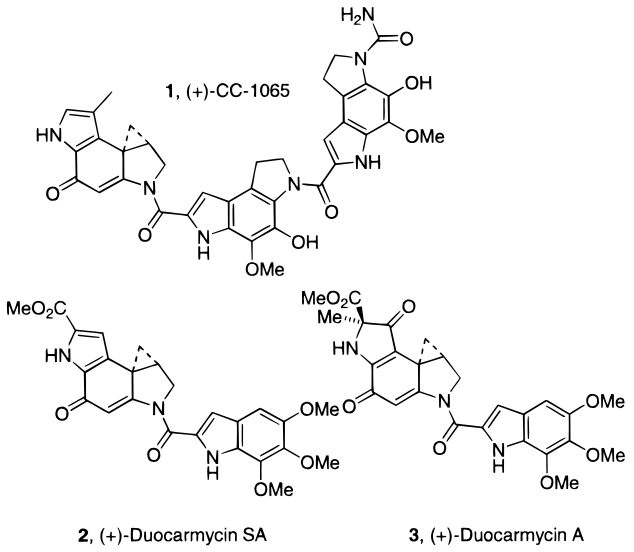

Figure 1.

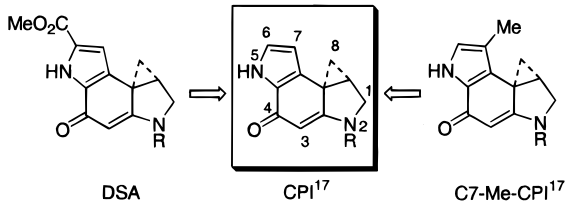

Figure 2.

sis of reversed analogues of duocarmycin SA,[7] and supporting evidence has been derived through solution structural studies[8,9] of the DNA adducts and the synthesis of carefully designed analogues containing deep-seated structural modifications.[10−16]

Herein, we describe the synthesis of 1,2,8,8a-tetrahydrocyclopropa[*c*]pyrrolo[3,2-*e*]indol-4(5*H*)-one (CPI),[17] the parent alkylation subunit of both duocarmycin SA and CC-1065 which lacks the C6 methoxycarbonyl and C7 methyl group of the respective natural products (Figure 2). The removal of the C6 methyl ester from the duocarmycin SA alkylation subunit leads to a decrease in the rigid length of the agent and should decrease the rate of DNA alkylation derived from catalysis by the binding-induced conformational change. The removal of the C7 methyl group from the alkylation subunit of CC-1065 (C7-MeCPI)[17] has not been previously investigated, and its role has been the subject of much speculation. Because this substituent protrudes into the floor of the minor groove, it was not clear whether this removal of the C7 methyl group would be a productive modification leading to an increase in DNA alkylation due to the removal of a steric impediment to minor groove alkylation or detrimental leading to a decrease in reaction selectivity or regioselectivity.

Scheme 1

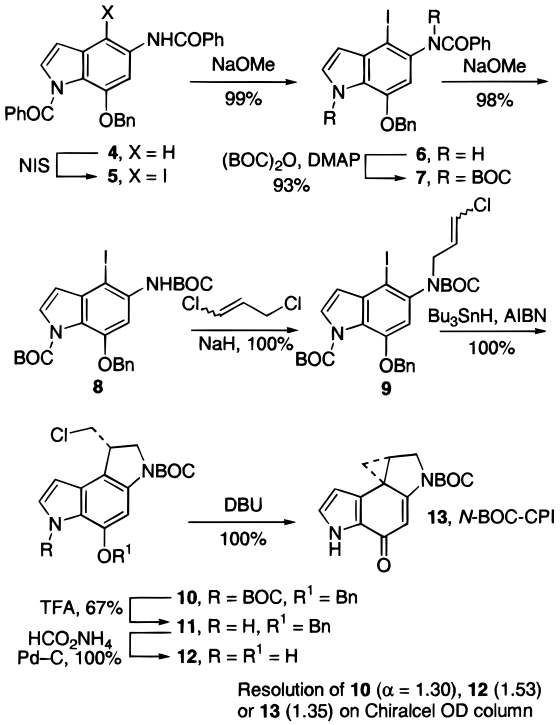

The studies described herein demonstrate that the duocarmycin SA C6 methoxycarbonyl conveys several productive features to the molecule. In addition to enhancing intrinsic chemical stability (6×) which results in a comparable enhancement in biological potency, it increases the rate of DNA alkylation approximately 12−13-fold and the alkylation efficiency 10-fold without altering the characteristic sequence selectivity. In contrast, the C7 methyl group of the CC-1065 alkylation subunit does not appear to convey productive characteristics to the natural product or its analogues. The agents described herein lacking the C7 methyl group possessed a comparable reactivity and reaction selectivity but alkylated DNA with a faster rate and improved efficiency. Thus, the C7 methyl group appears to be counterproductive, and the CPI analogues lacking this substituent exhibited a biological potency approximately 2−10 times greater than the corresponding CC-1065 analogue.

Synthesis of *N*-BOC-CPI. Regioselective iodination (NIS, TsOH) of indole **4**,[18] first prepared in synthetic efforts on CC-1065 and available in two steps from di-*N*-benzoyl-2-(benzyloxy)-*p*-quinonediimine, was followed by N^1-debenzoylation under basic conditions (2 M $NaOCH_3$, CH_3OH, 10 min, 25 °C, 99%) to provide **6** (Scheme 1). Further removal of the N^5-benzoyl group was

(7) Boger, D. L.; Bollinger, B.; Hertzog, D. L.; Johnson, D. S.; Cai, H.; Mésini, P.; Garbaccio, R. M.; Jin, Q.; Kitos, P. A. *J. Am. Chem. Soc.* **1997**, *119*, 4987.

(8) Eis, P. S.; Smith, J. A.; Rydzewski, J. M.; Case, D. A.; Boger, D. L.; Chazin, W. J. *J. Mol. Biol.* **1997**, *272*, 237.

(9) Schnell, J. R.; Ketchem, R. R.; Boger, D. L.; Chazin, W. J. *J. Am. Chem. Soc.* **1999**, *121*, 5645.

(10) Boger, D. L.; Hertzog, D. L.; Bollinger, B.; Johnson, D. S.; Cai, H.; Goldberg, J.; Turnbull, P. *J. Am. Chem. Soc.* **1997**, *119*, 4977.

(11) Boger, D. L.; Garbaccio, R. M.; Jin, Q. *J. Am. Chem. Soc* **1997**, *62*, 8875.

(12) Boger, D. L.; Santillán, A., Jr; Searcey, M.; Jin, Q. *J. Am. Chem. Soc.* **1998**, *120*, 11554.

(13) Boger, D. L.; Santillán, A., Jr.; Searcey, M.; Jin, Q. *J. Org. Chem.* **1999**, *64*, 5241.

(14) Boger, D. L.; Turnbull, P. *J. Org. Chem.* **1997**, *62*, 5849.

(15) Boger, D. L.; Turnbull, P. *J. Org. Chem.* **1998**, *63*, 8004.

(16) Boger, D. L.; Garbaccio, R. M. *J. Org. Chem.* **1999**, *64*, 5666.

(17) In preceding studies, CPI has been used as an abbreviation for the CC-1065 alkylation subunit. Since it more accurately reflects the abbreviation for the parent unsubstituted alkylation subunit described herein, we have adopted CPI as its abbreviation and C7-MeCPI for the CC-1065 alkylation subunit.

(18) Boger, D. L.; Zarrinmayeh, H. *J. Org. Chem.* **1990**, *55*, 1379.

Table 1. Resolution on Chiralcel OD Column

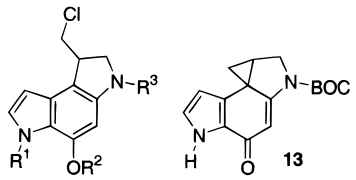

13

agent	R^1	R^2	R^3	α
10	BOC	Bn	BOC	1.30
11	H	Bn	BOC	1
12	H	H	BOC	1.53
13	–	–	–	1.35

accomplished by treatment of **6** with BOC_2O and DMAP at room temperature for 30 min (93%), followed by hydrolysis of the benzoyl group (2 M $NaOCH_3$, CH_3OH, 10 min, 25 °C, 98%). Intermediate **8** was *N*-alkylated to give the key substrate **9** for free radical cyclization (3 equiv of NaH, 3 equiv of 1,3-dichloropropene, DMF, 1 h, 25 °C, 100%).[19] The cyclization occurred smoothly in toluene (90 °C, 0.1 equiv of AIBN, 1 equiv of Bu_3SnH, 1 h, 100%) to give **10**, the fully protected precursor to *N*-BOC-CPI. This free radical reaction could also be conducted with catalytic amounts of tin and treatment of **9** with $(Bu_3Sn)_2O$ (0.1 equiv) and poly(methylhydroxysiloxane) (PMHS) under conditions described by Fu and co-workers[20] cleanly provided **10** (55%).

Although not integral to the preparation of advanced CPI analogues where both the N^1 and N^5 BOC protecting groups are removed simultaneously, the preparation of *N*-BOC-CPI itself required selective removal of the indole N^1-BOC group. This could be achieved under mild acidic conditions (TFA, CH_2Cl_2, 1−2 h, 0 to 25 °C, 67%, typically 65−80%) providing **11**. Debenzylation using transfer hydrogenation[21] (25% aq HCO_2NH_4, THF, 10% Pd/C, 2 h, 25 °C, 100%) followed by spirocyclization (DBU, CH_3CN, 25 °C, 10 min, 100%) gave *N*-BOC-CPI in excellent conversions. In fact, spirocyclization was so facile that purification of **12** by SiO_2 chromatography often resulted in partial closure to **13**.[22] This same route was also explored using the corresponding bromide derived from treatment of **4** with NBS and found to give comparable conversions, including that of the 5-*exo*-*trig* free radical cyclization.[19]

In conjunction with efforts to establish the properties of the *O*-benzyl-protected CPI derivatives, we examined the possibility that **11** and related agents may spirocyclize via participation of the indole N^5-H (eq 1). Analogous observations with KW-2189 have been made although in this case the indole NH is much more acidic and the leaving group (Br vs Cl) more reactive.[23] Thus, while KW-2189 was found to undergo solvolysis and alkylate DNA albeit less effectively than the free phenol,[23] **11** failed to provide evidence of spirocyclization and was recovered unchanged upon treatment with NaH (THF), DBU (CH_3CN), $Et_3N-CH_3CN-H_2O$ (1:1:1), or pH 7 phosphate buffer. While this was only examined in preliminary experiments which do not preclude such behavior, it is suggestive that the spirocyclization of **11** and related agents is not facile and unlikely to be significant.

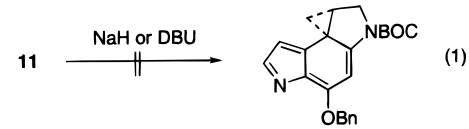

Resolution. To assess the properties of both enantiomers of the CPI-based agents, direct chromatographic resolution of **10**−**13** on a Chiralcel OD semipreparative HPLC column (2 × 25 cm, 10% *i*-PrOH-hexane eluent, 7 mL/min) was investigated (Table 1). Compound **10**, the product of the free radical cyclization and immediate precursor to the extended analogues, was effectively resolved (α = 1.30). Although compound **11** was incapable of resolution under similar conditions, the intermediate **12** could also be resolved with excellent separation of the enantiomers (α = 1.53), as could *N*-BOC-CPI (**13**, α = 1.35). The absolute configuration was assigned on the basis of the DNA alkylation selectivity of the analogues prepared from the two enantiomers and was consistent with expected $[\alpha]_D$ rotation values, relative Chiralcel OD retention times, and cytotoxic potency.

Solvolysis: Reactivity. The relative reactivity of the alkylation subunits as established by their rate of acid-catalyzed solvolysis has been found to reflect a direct relationship between stability and in vitro biological potency.[3] The solvolysis of *N*-BOC-CPI at pH 3.0 (50% CH_3OH−buffer, buffer = 4:1:20 v/v/v 0.1 M citric acid, 0.2 M Na_2HPO_4, H_2O) was followed spectrophotometrically by UV with the disappearance of the long wavelength absorption at 343 nm of the CPI chromophore and with the appearance of a short wavelength absorption at 238 nm attributable to the solvolysis product. The reactivity of *N*-BOC-CPI ($k = 7.13 \times 10^{-6}$ s^{-1}, $t_{1/2} = 27$ h) was similar to the BOC derivative of the CC-1065 alkylation subunit ($t_{1/2} = 37$ h) but substantially greater (6−7×) than the duocarmycin SA alkylation subunit *N*-BOC-DSA ($t_{1/2} = 177$ h), Figure 3. This indicates that the C7 methyl group of the CC-1065 alkylation subunit has little effect on the acid-catalyzed solvolysis reactivity, whereas the electron-withdrawing nature of the duocarmycin SA C6 methyl ester has a stabilizing effect.

Solvolysis: Regioselectivity. The acid-catalyzed nucleophilic addition of CH_3OH to *N*-BOC-CPI was conducted on a preparative scale to establish the regioselectivity of addition. Treatment of **13** with catalytic CF_3SO_3H (0.12 equiv, CH_3OH, 0−25 °C, 3 h, 90%) led to two products in a ratio of 4:1 (Scheme 2). The major product **21** results from attack at the least-substituted cyclopropane carbon, and the addition occurs with a regioselectivity identical to that of the natural product alkylation subunits.[24,25] The minor ring expansion prod-

(19) Patel, V. F.; Andis, S. L.; Enkema, J. K.; Johnson, D. A.; Kennedy, J. H.; Mohamadi, F.; Schultz, R. M.; Soose, D. J.; Spees, M. M. *J. Org. Chem*. **1997**, *62*, 8868. Boger, D. L.; Boyce, C. W.; Garbaccio, R. M.; Searcey, M. *Tetrahedron Lett.* **1998**, *39*, 2227.

(20) Lopez, R. M.; Hays, D. S.; Fu, G. C. *J. Am. Chem. Soc.* **1997**, *119*, 6949.

(21) Ram. S.; Ehrenkaufer, R. E. *Synthesis* **1988**, 91.

(22) Efforts to further shorten this route by reacting **5** with BOC_2O (25 °C, 91%) followed by treatment of the resulting imide with 2 M $NaOCH_3-CH_3OH$ (25 °C, 4 h, 91%) provided 7-(benzyloxy)-5-[(*tert*-butyloxycarbonyl)amino]-4-iodoindole cleanly. However, attempts to alkylate N^5 selectively with 1,3-dichloropropene provided mixtures of N^1 and N^5 alkylation. Similarly, although this was not investigated in detail, attempted alkylation of **5** with 1,3-dichloropropene failed to provide the *N*-alkylated material cleanly.

(23) Asai, A.; Nagamura, S.; Saito, H. *J. Am. Chem. Soc.* **1994**, *116*, 4171.

(24) Warpehoski, M. A.; Harper, D. E. *J. Am. Chem. Soc.* **1994**, *116*, 7573. Warpehoski, M. A.; Harper, D. E. *J. Am. Chem. Soc.* **1995**, *117*, 2951.

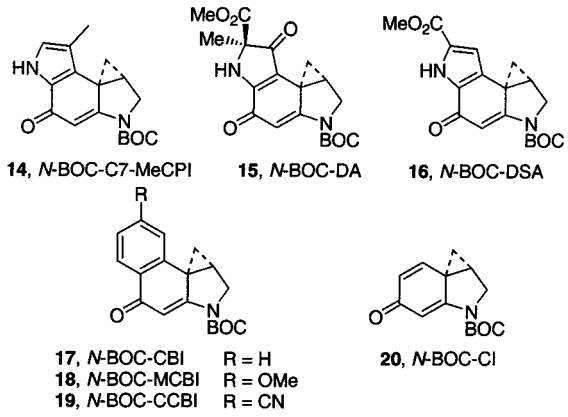

agent	k (s^{-1}, pH 3)	$t_{1/2}$ (h, pH 3)	regioselectivity
13	7.13×10^{-6}	27	4 : 1
14	5.26×10^{-6}	37	4 : 1
15	1.75×10^{-5}	11	3 : 2
16	1.08×10^{-6}	177	6–4 : 1
17	1.45×10^{-6}	133	> 20 : 1
18	1.75×10^{-6}	110	> 20 : 1
19	0.99×10^{-6}	194	> 20 : 1
20	1.98×10^{-2}	0.01	nd

Figure 3.

Scheme 2

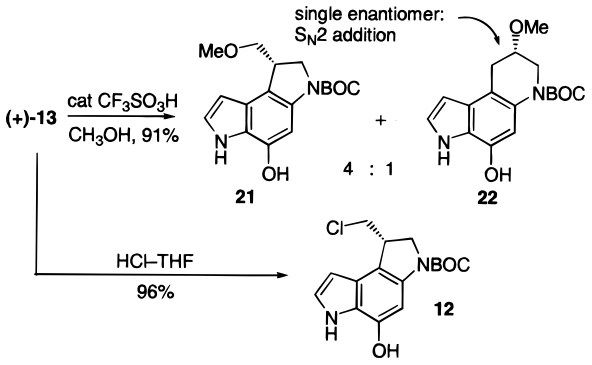

uct **22** was found to be generated exclusively with inversion of the reacting center stereochemistry, indicating that the attack of methanol occurs by clean S_N2 addition (see Experimental Section). This is analogous to our observations with *N*-BOC-DSA,[10,25] *N*-BOC-DA,[25] and related agents,[14,16] but contrasts the purported behavior of C7-MeCPI reported by Warpehoski[24] and disclosed without such conclusive evidence of the extent of maintenance or loss of stereochemistry. Treatment of *N*-BOC-CPI with HCl in THF (1.8 equiv, −78 °C) cleanly gave only the product of addition to the less-substituted cyclopropane, with no trace of formation of the ring-expanded product. Identical observations have been described for the natural alkylation subunits of CC-1065 and the duocarmycins,[10,23−25] and results from the increased preference for S_N2 addition to the least-substituted carbon by large nucleophiles. Thus, the removal of the CC-1065 C7 methyl group or the duocarmycin SA C6 methoxycarbonyl group has no impact on the intrinsic reaction regioselectivity.

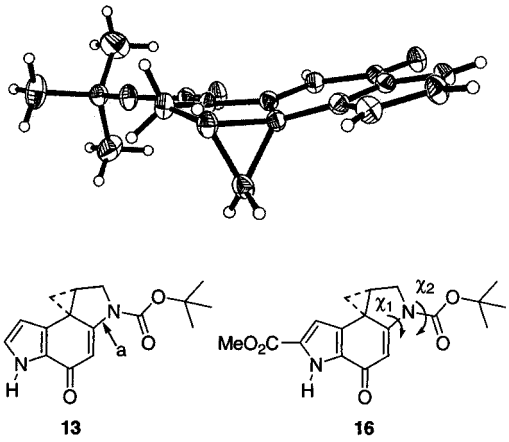

X-ray bond length, Å	*N*-BOC-CPI (13)	*N*-BOC-DSA (16)
a	1.396	1.393
X-ray dihedral angle		
χ_1	12.6°	6.9°
χ_2	6.3°	4.5°

Figure 4.

X-ray Crystal Structure of *N*-BOC-CPI and Relationships to Reactivity and Reaction Regioselectivity.[26] The single-crystal X-ray structures of the alkylation subunits of CC-1065, the duocarmycins, and synthetic analogues have provided insights into the origins of their reaction regioselectivity and differences in stability.[3,6] The stability of the alkylation subunits is a result of three structural features: the conjugative stability provided by the fused aromatic ring, the nonideal alignment of the cyclopropane, and the cross-conjugative stability provided by the vinylogous amide with the latter being especially important. The difference in reactivity of ring-expanded analogues of CBI (i.e., CBQ and CNA)[14,16] has been accurately correlated with an increase in the bond length *a* and in the torsion angle χ_1 diagnostic of the extent of vinylogous amide cross conjugation. This bond length and χ_1 torsion angle for *N*-BOC-CPI were 1.396 Å and 12.6°. These values are close to those of *N*-BOC-DSA (1.393 Å, 6.9°) but diagnostic of less vinylogous amide conjugation, indicating that the increased reactivity of CPI alkylation subunit may stem in part from the decrease in cross conjugation of the vinylogous amide (Figure 4). Further contributing to the differences in reactivity is the electronic nature of the pyrrole ring substitution arising from removal of the electron-withdrawing methoxycarbonyl group of *N*-BOC-DSA. The comparable stereoelectronic alignment of the CPI and DSA cyclopropanes with the cyclohexadienone π-system accounts for their near identical reaction regioselectivity.

Synthesis of Key Duocarmycin and CC-1065 Analogues. Coupling of the CPI alkylation subunit to the DNA binding subunits of duocarmycin, CC-1065, and related analogues followed a general procedure previously reported[19] (Scheme 3). This approach was especially attractive because of the successful resolution of the early synthetic intermediate **10**. Exhaustive BOC deprotection

(25) Boger, D. L.; Goldberg, J.; McKie, J. A. *Bioorg. Med. Chem. Lett.* **1996**, *6*, 1955. Boger, D. L.; McKie, J. A.; Nishi, T.; Ogiku, T. *J. Am. Chem. Soc.* **1997**, *119*, 311.

(26) The atomic coordinates for this structure have been deposited with the Cambridge Crystallographic Data Centre and may be obtained upon request from the Director, Cambridge Crystallographic Data Centre, 12 Union Road, Cambridge, CB2 1EZ, UK.

Scheme 3

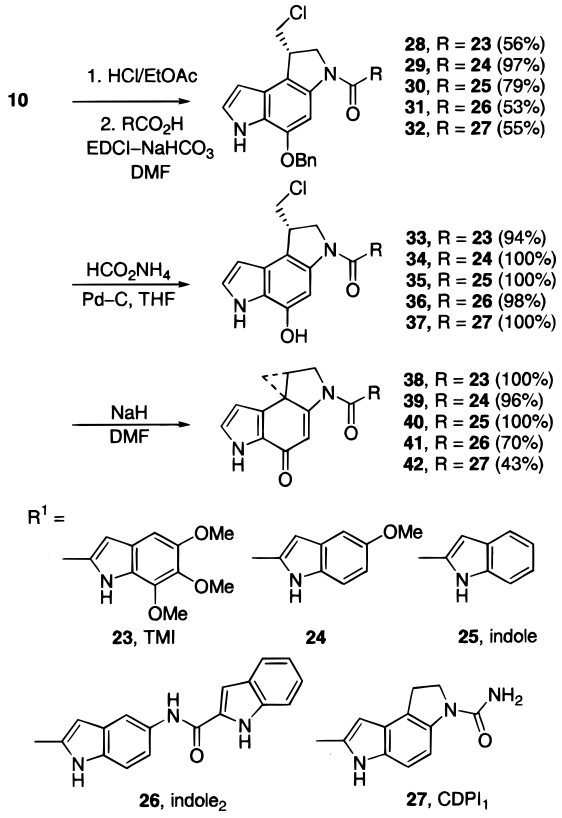

(3.6 M HCl/EtOAc, 25 °C, 30 min) of **10** followed by immediate coupling of the amine hydrochloride (3 equiv of EDCI, 5 equiv of $NaHCO_3$, DMF, 53−97%) with the appropriate carboxylic acid (1.2 equiv of **23**−**27**) provided the benzyl protected *seco*-CPI derivatives **28**−**32** in good yields. Debenzylation (25% aq HCO_2NH_4, 10% Pd/C, THF, 94−100%) followed by base-catalyzed ring closure (3 equiv of NaH, DMF, 43−100%) provided the desired products **38**−**42**. The advantages of proceeding through the benzyl-protected *seco*-CPI agents are severalfold. Purification of the coupled products was facilitated by the relative nonpolar properties and favorable solubility characteristics of the intermediate. Typically purification of the coupling products derived from **12** were contaminated with the corresponding cyclopropane agents which formed upon SiO_2 purification. Thus, purifications of **28**−**32** followed by their deprotection provided **33**−**37** sufficiently clean as to not require further purification. In addition, comparable attempts to couple the phenol derived from deprotection of **12** proved less successful and sometimes problematic. Finally and more importantly, the benzyl-protected precursors **28**−**32** are relatively nontoxic compared to **33**−**37**, constituting easily purified and readily stored intermediates.

DNA Alkylation Selectivity and Efficiency. The DNA alkylation properties of the agents were examined within w794 duplex DNA for which comparison results are available for related agents. The alkylation site identification and the assessment of the relative selectivity among the available sites were obtained by thermally induced strand cleavage of the singly 5′-end-labeled duplex DNA after exposure to the agents. Following treatment of the end-labeled duplex DNA with a range of agent concentrations, the unbound agent was removed by ethanol precipitation of the DNA. Redissolution of the DNA in aqueous buffer, thermolysis (100 °C, 30 min) to induce strand cleavage at the sites of alkylation, denaturing polyacrylamide gel electrophoresis (PAGE) adjacent to Sanger sequencing lanes, and autoradiography led to identification of the DNA cleavage and alkylation sites. The full details of this procedure have been disclosed elsewhere.[27] A representative comparison of DNA alkylation by (+)-CPI-TMI (**38**), (+)-**39**, and (+)-CPI-indole (**40**) alongside (+)-duocarmycin SA within w794 is illustrated in a Supporting Information figure (Figure S1). All three of the (+)-CPI-derivatives alkylate DNA with selectivities identical to (+)-duocarmycin SA,[28,29] but with increasingly decreased efficiency (Table 2). Both (+)-**38** and (+)-**39** alkylate with an efficiency that is 10−50× less than the natural product. This behavior is additionally magnified with the further incremental loss of DNA alkylation efficiency seen with (+)-CPI-indole (ca. 100×), in which both the C6 methyl ester and the C5′ methoxy group of (+)-duocarmycin SA have been removed. This decrease in alkylation rate and efficiency is analogous to that observed while examining the role of the duocarmycin SA C5′ methoxy group (Table 2).[7,30] The behavior of CPI-indole (**40**) illustrates that both the C6 methoxycarbonyl group and the C5′ methoxy group independently contribute significantly to the DNA alkylation efficiency consistent with a potential role in activation derived from a DNA binding-induced conformational change. In this regard, it is notable that a similar observation within a series of CBI-based analogues (i.e., **17**−**19**) revealed that the increase in DNA alkylation efficiency and rate was not dependent upon the electronic character of the analogous C7 substituent, but rather related simply to its presence (**19** = **18** > **17,** CN = OCH_3 > H).[31]

Table 2. Relative Alkylation Efficiency[a]

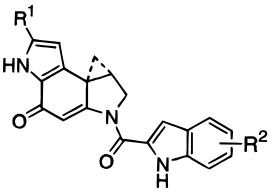

agent	R^1	R^2	relative alkylation efficiency
2	CO_2CH_3	5,6,7-OCH_3	1
	CO_2CH_3	5-OCH_3	1
	CO_2CH_3	H	0.05
38	H	5,6,7-OCH_3	0.1
39	H	5-OCH_3	0.1−0.05
40	H	H	0.01

[a] At the w794 high affinity site 5′-AATTA.

The CPI unnatural enantiomer DNA alkylation is considerably slower and was observed only after a more prolonged incubation (72 versus 24 h, 25 °C, Supporting

(27) Boger, D. L.; Munk, S. A.; Zarrinmayeh, H.; Ishizaki, T.; Haught, J.; Bina, M. *Tetrahedron* **1991**, *47*, 2661.
(28) Boger, D. L.; Johnson, D. S.; Yun, W. *J. Am. Chem. Soc.* **1994**, *116*, 1635. Boger, D. L.; Johnson, D. S.; Yun, W.; Tarby, C. M. *Bioorg. Med. Chem.* **1994**, *2*, 115.
(29) Boger, D. L.; Ishizaki, T.; Zarrinmayeh, H.; Munk, S. A.; Kitos, P. A.; Suntornwat, O. *J. Am. Chem. Soc.* **1990**, *112*, 8961. Boger, D. L.; Coleman, R. S.; Invergo, B. J.; Sakya, S. M.; Ishizaki, T.; Munk, S. A.; Zarrinmayeh, H.; Kitos, P. A.; Thompson, S. C. *J. Am. Chem. Soc.* **1990**, *112*, 4263.
(30) Boger, D. L.; Bollinger, B.; Johnson, D. S. *Bioorg. Med. Chem. Lett.* **1996**, *6*, 2207.
(31) Boger, D. L.; Han, N.; Tarby, C.; Boyce, C. W.; Cai, H.; Jin, Q.; Kitos, P. A. *J. Org. Chem.* **1996**, *61*, 4894.

Information Figure S1). Even with the longer reaction times, the alkylation by the unnatural enantiomers is less efficient, requiring higher agent concentrations to detect. The DNA alkylation selectivity observed with *ent*-(−)-CPI-TMI and *ent*-(−)-duocarmycin SA was indistinguishable but, consistent with the observations made with the natural enantiomers, the efficiency of alkylation by (−)-CPI-TMI was less (50−100×) than that of (−)-duocarmycin SA which possesses the more extended rigid structure. Thus, the incorporation of the C6 methoxycarbonyl group increased the unnatural enantiomer DNA alkylation even more significantly than the natural enantiomer. The alkyation sites for the unnatural enantiomers proved consistent with adenine N3 alkylation in the minor groove with the agent binding in the 5′ to 3′ direction across a 3.5 base pair AT-rich sequence surrounding the alkylation site.[32] This is analogous to the natural enantiomer alkylation selectivity which extends in the reverse 3′ to 5′ direction in the minor groove and, because of the diastereomeric nature of the adducts, is offset by one base pair relative to the natural enantiomers.[28]

Relative Rates of Alkylation for (+)-CPI-TMI (38), (+)-CPI-indole (40), and (+)-Duocarmycin SA (2). The relative rates of DNA alkylation for (+)-CPI-TMI (**38**), (+)-CPI-indole (**40**), and (+)-duocarmycin SA (**2**) at the w794 high affinity site were measured (25 °C, 24 h, 10^{-5} and 10^{-4} M), and the results are shown in Figure 5 and summarized in Table 3. In previous studies, the comparison of (+)-duocarmycin SA (**2**), (+)-DSA-5-methoxyindole, and (+)-DSA-indole established that the removal of the C5′ methoxy substituent leads to a substantial decrease in the relative alkylation rate.[7,30] The loss of this group, which extends the rigid length of the binding subunit, leads to a decrease in the inherent twist in the helical conformation of the DNA bound agent. The degree of twist in the N^2 amide induced upon binding contributes to the disruption of the vinylogous amide conjugation and the increase in the inherent reactivity of the agent, thus contributing to the catalysis of the DNA alkylation reaction. This effect on the rate of DNA alkylation is clearly demonstrated with the CPI-based agents. A decrease in the extended rigid length of duocarmycin SA through removal of the left-hand subunit C6 methyl ester leads to a 12−13× decrease in the relative rate of DNA alkylation. Thus, the C6 methoxycarbonyl group of duocarmycin SA contributes significantly to the rate of DNA alkylation. This is especially significant since **38** is intrinsically 6× more reactive than **2** yet alkylates DNA 12−13× slower. As reported previously, removal of the right-hand side C5′ methoxy group led to a 20× reduction in the rate of DNA alkylation.[7,30] Removing the groups on *both* the left and right-hand subunits leads to a 250× decrease in the relative alkylation rate, demonstrating the predicted cumulative effect (predict 240−260×) and highlighting the magnitude of these structural variations on the activation of the DNA bound agent.

Relative Rates and Efficiencies of Alkylation for (+)-CPI-indole$_2$ (41), 45, and (+)-DSA-indole$_2$ (43). A representative example of DNA alkylation by (+)-**41** within w794 is illustrated in Figure 6 and demonstrates

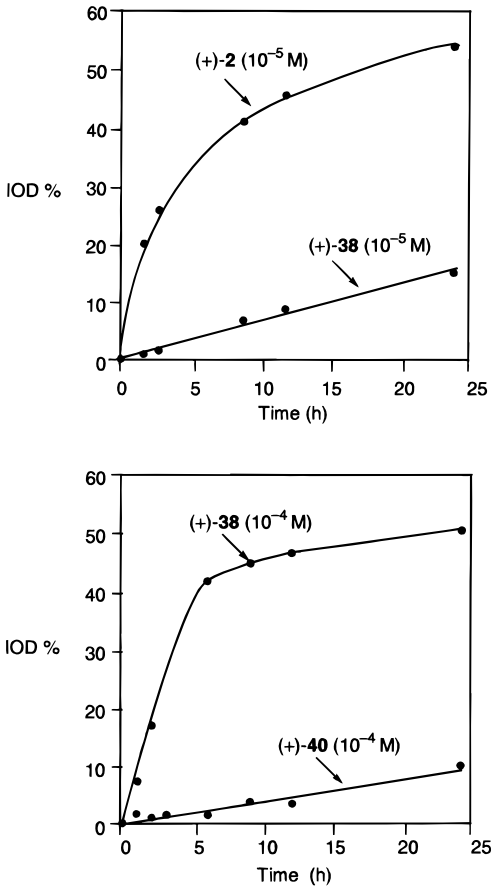

Figure 5. Plots of percent integrated optical density (% IOD) versus time established through autoradiography of 5′-^{32}P end-labeled DNA and used to monitor the relative rate of w794 DNA alkylation of the 5′-AATTA high affinity site for (+)-duocarmycin SA (**2**), (+)-**38** and (+)-**40**. Alkylation by (+)-**2** and (+)-**38** were compared at a concentration of 10^{-5} M and (+)-**38** and (+)-**40** were compared at 10^{-4} M, 25 °C.

Table 3. Relative Rates of DNA Alkylation[a]

agent	k_{rel}
Shortened Agents	
(+)-**2**, duocarmycin SA	1
(+)-**38**, CPI-TMI	0.08
(+)-DSA-indole	0.05
(+)-**40**, CPI-indole	0.004
Extended Agents	
(+)-**41**, CPI-indole$_2$	0.18
(+)-**43**, DSA-indole$_2$	1
(+)-**44**, CBI-indole$_2$	0.65
(+)-**45**, C7-MeCPI-indole$_2$	0.05

[a] At the w794 high affinity site 5′-AATTA.

the 10-fold decrease in alkylation efficiency of (+)-CPI-indole$_2$ (10^{-5} M) analogous to (+)-C7-MeCPI-indole$_2$[33] compared with (+)-DSA-indole$_2$ which alkylates the same single high affinity site in w794 DNA at 10^{-6} M concentration. The relative rates of alkylation for (+)-CPI-indole$_2$ (**41**), (+)-CBI-indole$_2$ (**44**), and (+)-DSA-indole$_2$ (**43**) at the w794 high affinity site were measured (25 °C, 24 h, 10^{-5} M agent concentration), and the results are shown in Figure 7 and summarized in Table 3. In previous studies, the relative rates of alkylation for (+)-**43**−**45** were measured, and while the DSA and CBI

(32) The exceptions to this constitute alkylation sites observed for the contaminate natural enantiomer (<1%) which alkylates DNA more rapidly and efficiently.

(33) Boger, D. L.; Ishizaki, T.; Sakya, S. M.; Munk, S. A.; Kitos, P. A.; Jin, Q.; Besterman, J. M. *Bioorg. Med. Chem. Lett.* **1991**, *1*, 115.

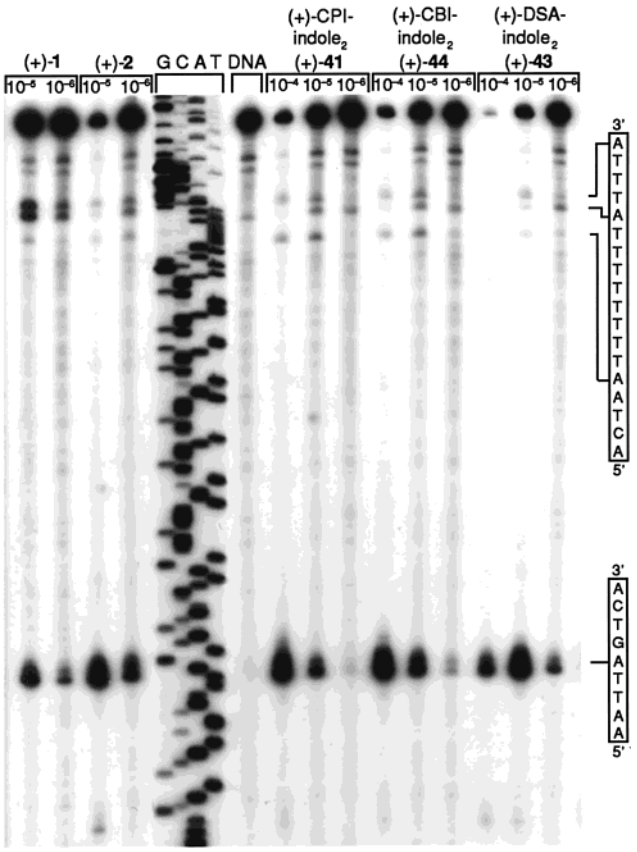

Figure 6. Thermally induced strand cleavage of w794 DNA (SV40 DNA segment, 144 bp, nucleotide no. 138-5238); DNA-agent incubation for 24 h at 25 °C, removal of unbound agent and 30 min of thermolysis (100 °C), followed by denaturing 8% PAGE and autoradiography; lanes 1 and 2, (+)-CC-1065 (**1**, 1×10^{-5} and 1×10^{-6} M); lanes 3 and 4, (+)-duocarmycin SA (**2**, 1×10^{-5} and 1×10^{-6} M); lanes 5−8, Sanger G, C, A and T sequencing reactions; lane 9, control DNA; lanes 10−12, (+)-CPI-indole$_2$ (**41**, 1×10^{-4} to 1×10^{-6} M); lanes 13−15, (+)-CBI-indole$_2$ (**44**, 1×10^{-4} to 1×10^{-6} M); lanes 16−18, (+)-DSA-indole$_2$ (**43**, 1×10^{-4} to 1×10^{-6} M).

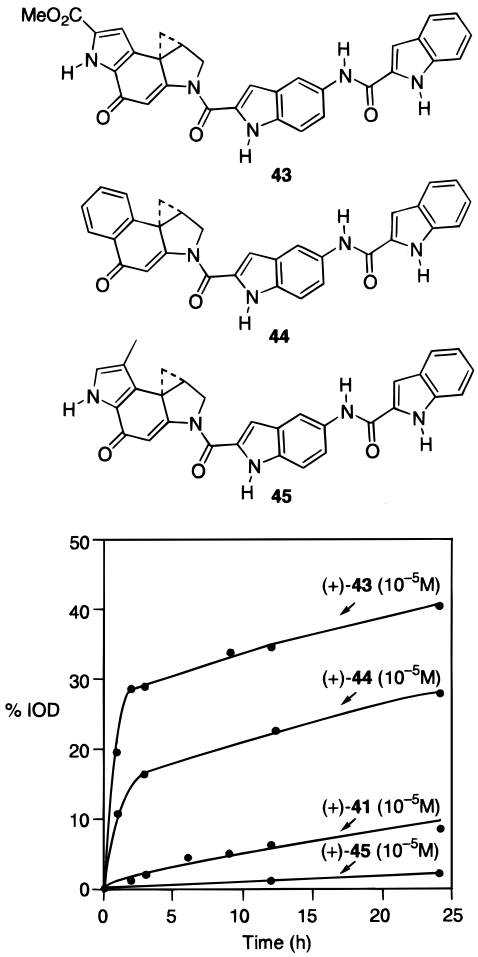

Figure 7. Plots of percent integrated optical density (% IOD) versus time established through autoradiography of 5′-^{32}P end-labeled DNA and used to monitor the relative rate of w794 alkylation of the 5′-AATT*A* high affinity site for (+)-DSA-indole$_2$ (**43**), (+)-CBI-indole$_2$ (**44**), (+)-CPI-indole$_2$ (**41**) and (+)-C7-MeCPI-indole$_2$ (**45**) at a concentration of 10^{-5} M compound, 25 °C. The relative rates of alkylation are as follows: (+)-DSA-indole$_2$ (21.5×) > (+)-CBI-indole$_2$ (14.0×) > (+)-CPI-indole$_2$ (4.0×) > (+)-C7-MeCPI-indole$_2$ (1.0×).

agents were similar in reactivity with DSA-indole$_2$ having a rate 1.5−2.0× faster than that of CBI-indole$_2$, the CC-1065 alkylation subunit analogue reacted much more slowly with a rate 14−15× less than that of CBI-indole$_2$ despite its greater intrinsic reactivity.[31] To define the effect of the CC-1065 C7 methyl substituent on the DNA alkylation rate, CPI-indole$_2$ (**41**) was compared with the preceding agents. Its relative rate of DNA alkylation was established to be faster than that of C7-MeCPI-indole$_2$ (**45**). The absence of the C7 methyl substituent, which has been suggested to contribute either a steric impediment to the binding and positioning of the alkylating agent in the minor groove or to contribute to the selectivity of alkylation by precluding unproductive alkylations, was found to slow the relative alkylation rate, with (+)-**45** having a rate 4× slower than **41** and >20× slower than DSA-indole$_2$. This indicates that the duocarmycin SA C6 methoxycarbonyl group enhances the rate of DNA alkylation 6× despite the fact that the alkylation subunit is intrinsically 6× less reactive and that the C7 methyl group of CC-1065 slows the relative DNA alkylation rate (4×) and lowers the efficiency of DNA alkylation.

Cytotoxic Activity. The compounds displayed cytotoxic activity consistent with their DNA alkylation properties and relative stabilities (Table 4). The CPI-based analogues were more potent than the corresponding analogue containing the CC-1065 alkylation subunit and were comparable or slightly less potent than the analogues containing the duocarmycin SA alkylation subunit. Instructive in this regard is the L1210 activity (IC_{50}) of the *N*-BOC derivatives *N*-BOC-CPI (**13**, 160 nM), *N*-BOC-C7-MeCPI (**14**, 330 nM), and *N*-BOC-DSA (**16**, 6 nM) and that of (+)-C7-MeCPI-indole$_2$ (**45**), (+)-CPI-indole$_2$ (**41**), and DSA-indole$_2$ (**43**): IC_{50} = 40, 3, and 3 pM, respectively. Like prior observations, the natural enantiomers were significantly more potent than the corresponding unnatural enantiomers (10−200×). However, the relative distinctions were typically larger than those observed with the DSA-based analogues (5−50×) and more similar to the differences observed with the CC-1065 analogues (1−1000×). Analogous to prior observations, the phenol precursors **33**−**37** displayed cytotoxic activity that was not distinguishable from the final agents containing the cyclopropane, indicating spirocyclization readily occurs under the conditions of the assay. The corresponding precursors in which the phenol is protected as the benzyl ether were substantially less potent (ca. 10−200×), but not inactive. Even these deriv-

Table 4. In Vitro Cytotoxic Activity

compd	IC_{50}, nM (L1210)[a]		compd	IC_{50}, nM (L1210)[a]	
natural enantiomers			unnatural enantiomers		
13, (+)-*N*-BOC-CPI	160	(210)	(−)-*N*-BOC-CPI	1000	(1000)
38, (+)-CPI-TMI	0.007	(0.008)	(−)-CPI-TMI	1	(1)
39, (+)-CPI-(5-MeO)indole	0.009	(0.008)	(−)-CPI-(5-MeO)indole	1	(10)
40, (+)-CPI-indole	0.050	(0.070)	(−)-CPI-indole	10	(70)
41, (+)-CPI-indole$_2$	0.003	(0.002)	(−)-CPI-indole$_2$	1	(1)
42, (+)-CPI-CDPI$_1$	0.009	(0.009)	(−)-CPI-CDPI$_1$	2	(4)
1, (+)-CC-1065	0.020		(−)-CC-1065	0.020	
2, (+)-duocarmycin SA	0.006		(−)-duocarmycin SA	0.100	
14, (+)-*N*-BOC-C7-MeCPI	330				
16, (+)-*N*-BOC-DSA	6		(−)-*N*-BOC-DSA	60	
			O-benzyl derivatives		
28	0.1			50	
29	0.1			50	
30	nd			100	
31	0.5			100	
32	1.3			20	

[a] The value in parentheses is the IC_{50} for the corresponding seco derivatives **12**, **33**−**37**. The assays were conducted at least four times, and the average IC_{50} is reported; see ref 2.

atives retain significant activity, with the natural enantiomers exhibiting IC_{50}'s of ca. 0.1−1 nM, and the unnatural enantiomers were again less potent (20−100 nM).

Conclusions. A concise synthesis of the parent CPI alkylation subunit is described which lacks the C6 methoxycarbonyl group of duocarmycin SA and the C7 methyl group of CC-1065. The evaluation of its properties revealed that the duocarmycin SA C6 methyl ester substantially increases stability (6×) while the CC-1065 C7 methyl group has no or only a relatively small effect on the alkylation subunit reactivity. Neither substituent has any impact on the intrinsic reaction regioselectivity of the activated cyclopropane. Most remarkable is the effect of the substitution pattern on the reactivity of the agents toward DNA alkylation. The duocarmycin SA C6 methoxycarbonyl group substantially increases both the efficiency and rate of DNA alkylation despite its intrinsic greater stability, without altering the inherent sequence selectivity, while the CC-1065 C7 methyl group slows the rate and lowers the efficiency of DNA alkylation. The removal of the methoxycarbonyl group and the resulting decrease in rigid length in going from duocarmycin SA to CPI-TMI (**38**) leads to a 12−13-fold decrease in the relative rate of DNA alkylation. A similar effect has been previously described for DSA-indole, in which removal of the C5′ methoxy substituent on the right-hand subunit led to a 20-fold decrease in the rate of DNA alkylation.[7,21] The even larger 250-fold decrease in alkylation rate seen with CPI-indole (**40**) in which *both* substituents are removed is the predicted product of the incremental decreases resulting from removal of each substituent. We have interpreted this behavior to lend further support for the model of agent activation derived from a DNA binding-induced twist in the linking amide disrupting the stabilizing vinylogous amide cross-conjugation. The duocarmycin SA C6 methyl ester and C5′ methoxy group lie deep in the minor groove, increasing the rigid length of the agent and thus the degree of the binding-induced twist. Their removal decreases the degree of activation leading to the slower and less-efficient DNA alkylation. In contrast, the CC-1065 C7 methyl substituent was found to slow the rate of DNA alkylation 4× and lower the efficiency of DNA alkylation without affecting the reaction selectivity or regioselectivity. Presumably this arises from steric interactions with the minor groove floor which hinder binding and alkylation. Consistent with these observations, the CC-1065 C7 methyl group diminishes the biological potency relative to the CPI-based agents.

Experimental Section

1-Benzoyl-5-(benzoylamino)-7-(benzyloxy)-4-iodoindole (5). A solution of indole **4**[17] (118 mg, 0.26 mmol) and TsOH (26 mg, 0.13 mmol) in THF (1 mL) was cooled to 0 °C and treated with NIS (71 mg, 0.312 mmol) in THF (1 mL). The reaction was allowed to warm to 25 °C. After 16 h, additional NIS (15 mg, 0.065 mmol) was added and the reaction was stirred for 24 h. The reaction mixture was diluted with 10% aqueous $NaHCO_3$ and extracted with $CHCl_3$. The organic layers were combined, dried ($MgSO_4$), and concentrated. Flash chromatography (SiO_2, 2.5 × 15 cm, 30% EtOAc/hexane) afforded **5** (67 mg, 45%) as a yellow solid: mp 148 °C; ^{1}H NMR ($CDCl_3$, 400 MHz) δ 8.15 (s, 1H, NH), 7.99 (d, J = 6.0 Hz, 2H), 7.64 (d, J = 8.0 Hz, 2H), 7.58−7.47 (m, 4H), 7.30−7.17 (m, 5H), 6.58 (d, J = 2.8 Hz, 1H), 4.92 (s, 2H); ^{13}C NMR ($CDCl_3$, 62.5 MHz) δ 167.9, 165.4, 147.2, 136.2, 135.8, 134.8, 134.7, 134.1, 132.9, 132.1, 129.8, 129.5, 128.9, 128.4, 128.2, 127.8, 127.7, 127.1, 122.4, 110.6, 102.1, 71.8, 70.5; FABHRMS (NBA/CsI) 704.9677 (M^+ + Cs, $C_{29}H_{21}IN_2O_3$ requires 704.9651). Anal. Calcd for $C_{29}H_{21}IN_2O_3$: C, 60.85; H, 3.70; N, 4.89. Found: C, 60.81; H, 3.73; N, 4.80.

5-(Benzoylamino)-7-(benzyloxy)-4-iodoindole (6). Compound **5** (1.60 g, 2.80 mmol) in CH_2Cl_2 (28 mL) was treated with $NaOCH_3$ in CH_3OH (2 M, 4.2 mL, 8.4 mmol), and the solution was stirred at 25 °C for 10 min. H_2O and EtOAc were added, and the organic layer was separated, dried ($MgSO_4$), and concentrated. Flash chromatography (SiO_2, 3 × 30 cm, 25% EtOAc/hexanes) afforded **6** (1.3 g, 99%) as a colorless solid: mp 165−166 °C; ^{1}H NMR ($CDCl_3$, 400 MHz) δ 8.61 (s, 1H), 8.31 (s, 1H), 8.05 (s, 1H), 8.00 (d, J = 6.8 Hz, 1H), 7.53 (m, 5H), 7.37 (m, 3H), 7.21 (dd, J = 2.8, 1.4 Hz, 1H), 6.43 (dd, J = 2.7, 1.2 Hz, 1H), 5.28 (s, 2H); ^{13}C NMR ($CDCl_3$, 62.5 MHz) δ 165.7, 145.8, 136.5, 135.1, 132.7, 132.1, 132.0, 129.1, 128.8, 128.5, 128.3, 127.3, 124.6, 123.4, 106.9, 99.7, 72.7, 70.7; FABHRMS (NBA/CsI) m/z 600.9408 (M^+ + Cs, $C_{22}H_{17}IN_2O_2$ requires 600.9389). Anal. Calcd for $C_{22}H_{17}IN_2O_2$: C, 56.43; H, 3.66; N, 5.98. Found: C, 56.61; H, 3.63; N, 5.90.

***N*^{5},1-Bis(*tert*-butyloxycarbonyl)-5-(benzoylamino)-7-(benzyloxy)-4-iodoindole (7).** Compound **6** (255 mg, 0.54 mmol) in CH_2Cl_2 (6 mL) was treated with di-*tert*-butyl dicarbonate (687 mg, 3.16 mmol) and DMAP (128 mg, 1.04 mmol). After 30 min at 25 °C the solution was subjected directly to flash chromatography (SiO_2, 2 × 15 cm, 20% EtOAc/hexane) to give **7** (390 mg, 93%) as an oil: (R_f 0.80, SiO_2, 25% EtOAc/hexane); ^{1}H NMR ($CDCl_3$, 400 MHz) δ 7.81 (d, J = 6.9 Hz, 2H), 7.55 (d, J = 3.6 Hz, 1H), 7.45 (m, 5H), 7.31 (m, 3H), 6.82 (s, 1H), 6.57 (d, J = 3.6 Hz, 1H), 5.15 (s, 2H), 1.47 (s, 9H), 1.22 (s, 9H); ^{13}C NMR ($CDCl_3$, 62.5 MHz) δ 171.8, 171.4, 152.5,

148.9, 148.2, 137.8, 137.1, 136.9, 136.5, 131.6, 129.5, 128.6, 128.5, 128.3, 128.2, 127.7, 111.2, 109.6, 84.2, 83.7, 71.5, 60.5, 28.0, 27.8; FABHRMS (NBA/CsI) *m/z* 801.0402 (M^+ + Cs, $C_{32}H_{33}IN_2O_6$ requires 801.0438).

1-(*tert*-Butyloxycarbonyl)-5-[(*tert*-butyloxycarbonyl)-amino]-7-(benzyloxy)-4-iodoindole (8). Compound **7** (600 mg, 0.9 mmol) in CH_2Cl_2 (33 mL) was treated with $NaOCH_3$ in CH_3OH (2 M, 0.94 mL, 1.9 mmol). After 10 min at 25 °C, H_2O and EtOAc were added, and the organic layer was separated. The aqueous layer was washed with EtOAc, and the combined organic layers were dried ($MgSO_4$) and concentrated. Chromatography (SiO_2, 2 × 15 cm, 10−25% EtOAc/hexanes gradient) afforded **8** (496 mg, 98%) as a colorless oil: ^{1}H NMR ($CDCl_3$, 400 MHz) δ 7.83 (br s, 1H), 7.53 (m, 3H), 7.37 (m, 3H), 6.84 (br s, 1H), 6.45 (d, J = 3.4 Hz, 1H), 5.21 (s, 2H), 1.54 (s, 9H), 1.45 (s, 9H); ^{13}C NMR ($CDCl_3$, 62.5 MHz) δ 161.0, 152.9, 148.0, 136.7, 135.3, 129.0, 128.3, 128.2, 127.9, 127.8, 120.8, 110.4, 102.0, 98.0, 83.7, 71.0, 66.7, 28.3, 27.6; FABHRMS (NBA/CsI) *m/z* 697.0176 (M^+ + Cs, $C_{25}H_{29}IN_2O_5$ requires 697.0176). Anal. Calcd for $C_{25}H_{29}IN_2O_5$: C, 53.20; H, 5.18; N, 4.96. Found: C, 53.27; H, 5.26; N, 4.75.

5-(Benzyloxy)-1-(chloromethyl)-3,6-bis(*tert*-butyloxycarbonyl)-1,2-dihydro-3*H*-pyrrolo[3,2-*e*]indole (10). A solution of **9** (394 mg, 0.61 mmol) and AIBN (39 mg) in toluene (40 mL) was degassed with N_2 for 15 min. The solution was warmed to 90 °C, and Bu_3SnH (0.17 mL, 0.61 mmol) was added in 4 portions over 1 h. The solution was cooled and concentrated, and the residue was dissolved in EtOAc. Flash chromatography (SiO_2, 1 × 10 cm, 10% EtOAc/hexanes) afforded **10** (313 mg, 100%) as a colorless film: ^{1}H NMR ($CDCl_3$, 400 MHz) δ 7.74 (br s, 1H), 7.52 (m, 2H), 7.29 (m, 3H), 7.27 (m, 1H), 6.40 (d, J = 1 Hz, 1H), 5.20 (br s, 2H), 4.12 (m, 2H), 3.86 (m, 2H), 3.48, (t, J = 10 Hz, 1H), 1.57 (s, 9H), 1.47 (s, 9H); ^{13}C NMR ($CDCl_3$, 62.5 MHz) δ 161.0, 148.8, 140.9, 136.9, 130.1, 128.6, 128.2, 127.7, 121.5, 116.0, 103.6, 97.0, 83.3, 71.0, 53.1, 46.8, 45.6, 28.5, 28.3; FABHRMS (NBA/CsI) *m/z* 512.2094 (M^+, $C_{28}H_{33}ClN_2O_5$ requires 512.2078).

(−)-(1*S*)-10: $[\alpha]^{22}_D$ −11 (*c* 1.3, EtOAc).

(+)-(1*R*)-10: $[\alpha]^{22}_D$ +11 (*c* 1.4, EtOAc).

5-(Benzyloxy)-3-(*tert*-butyloxycarbonyl)-1-(chloromethyl)-1,2-dihydro-3*H*-pyrrolo[3,2-*e*]indole (11). A solution of **10** (100 mg, 0.2 mmol) in CH_2Cl_2 (18 mL) was stirred under N_2 and treated with CF_3CO_2H (0.115 mL, 1 mmol). After 30 min, a further portion of CF_3CO_2H (0.115 mL, 1 mmol) was added. After 1 h, $NaHCO_3$ (400 mg) was added. The solution was diluted with CH_2Cl_2, washed with H_2O, dried ($MgSO_4$), and concentrated. Flash chromatography (SiO_2, 2 × 15 cm, 10% EtOAc/hexanes) afforded pure **11** (54 mg, 67%) as a colorless film: ^{1}H NMR (acetone-d_6, 400 MHz) δ 8.38 (s, 1H), 8.00 (br s, 1H), 7.45 (m, 5H), 7.16 (dd, J = 2.7, 2.8 Hz, 1H), 6.84 (br s, 1H), 5.20 (br s, 2H), 4.10 (m, 2H), 3.98 (m, 2H), 3.50 (t, J = 10.4 Hz, 1H), 1.56 (s, 9H); ^{13}C NMR ($CDCl_3$, 62.5 MHz) δ 153.0, 141.9, 140.9, 130.2, 128.7, 127.4, 127.3, 126.6, 124.9, 124.1, 116.4, 102.1, 96.8, 77.8, 70.9, 49.3, 46.4, 41.6, 28.7; FABHRMS (NBA/CsI) *m/z* 412.1529 (M^+, $C_{23}H_{25}ClN_2O_3$ requires 412.1554).

3-(*tert*-Butyloxycarbonyl)-1-(chloromethyl)-5-hydroxy-1,2-dihydro-3*H*-pyrrolo[3,2-*e*]indole (12). Compound **11** (168 mg, 0.41 mmol), HCO_2NH_4 (25% aq, 2.2 mL), and 10% Pd/C (84 mg) were stirred in THF (10 mL), and Ar was bubbled through the solution for 15 min. The mixture was then vigorously stirred under Ar for 2 h. The solution was diluted with EtOAc, dried ($MgSO_4$), filtered, and concentrated. Chromatography (SiO_2, 2 × 15 cm, 25% EtOAc/hexane) afforded **12** (132 mg, 100%) as a colorless film: ^{1}H NMR (acetone-d_6, 400 MHz) δ 9.22 (br s, 1H), 7.35 (br s, 1H), 7.22 (t, J = 2.8 Hz, 1H), 7.19 (br s, 1H), 6.39 (dd, J = 2.1, 3.1 Hz, 1H), 4.09 (m, 1H), 3.97 (m, 2H), 3.89 (m, 1H), 3.68 (dd, J = 8.3, 10.8 Hz, 1H), 1.53 (s, 9H); IR (film) ν_{max} 3376, 2977, 1660, 1577 cm^{-1}; FABHRMS (NBA/NaI) *m/z* 323.1155 (M^+ + H, $C_{16}H_{19}ClN_2O_3$ requires 323.1162).

(−)-(1*S*)-12: $[\alpha]^{22}_D$ −12 (*c* 0.46, THF).

(+)-(1*R*)-12: $[\alpha]^{22}_D$ +12 (*c* 0.47, THF).

2-(*tert*-Butyloxycarbonyl)-1,2,8,8a-tetrahydrocyclopropa[*c*]pyrrolo[3,2-*e*]indol-4-one (*N*-BOC-CPI, 13). DBU (0.264 mL, 2.18 mmol) was added to a stirred solution of **12** (132 mg, 0.41 mmol) in anhydrous acetonitrile (13 mL). After 10 min, the solvent was removed and the residue was subjected directly to chromatography (SiO_2, 2 × 15 cm, 0−5% CH_3OH−$CHCl_3$ gradient) to afford **13** (122 mg, 100%) as a tan solid: mp 198 °C (decomp); ^{1}H NMR ($CDCl_3$, 400 MHz) δ 10.80 (br s, 1H, NH), 7.07 (dd, J = 2.8, 2.7 Hz, 1H), 6.45 (br s, 1H), 6.00 (dd, J = 2.5, 2.4 Hz, 1H), 3.96 (m, 2H), 2.75 (m, 1H), 1.57 (dd, J = 7.7, 3.8 Hz, 1H), 1.51 (s, 9H), 1.33 (t, J = 4.6 Hz, 1H); ^{13}C NMR ($CDCl_3$, 62.5 MHz) δ 178.5, 160.0, 152.1, 131.1, 129.2, 125.0, 109.0, 102.1, 83.0, 53.7, 32.7, 28.5, 27.1, 23.5; UV (THF) λ_{max} (ϵ) 319 (15500), 278 (23600), 209 (15600) nm; FABHRMS (NBA/NaI) *m/z* 287.1409 (M^+ + H, $C_{16}H_{18}N_2O_3$ requires 287.1400).

(+)-(8a*R*,7b*S*)-13: $[\alpha]^{22}_D$ +161 (*c* 0.19, acetone).

(−)-(8a*S*, 7b*R*)-13: $[\alpha]^{22}_D$ −160 (*c* 0.20, acetone).

Resolution. A solution of **12** (27 mg, 2.18 mmol) in 10% 2-propanol−hexane was resolved on a semipreparative Diacel Chiralcel OD column (10 μm, 2 × 25 cm) using 10% 2-propanol−hexane as eluent (7 mL/min). The effluent was monitored at 254 nm, and the enantiomers eluted with retention times of 27.0 and 41.7 min (α = 1.53). The fractions were collected and concentrated to afford (−)-(1*S*)-**12** (12 mg, 89%, >99% ee) and *ent*-(+)-(1*R*)-**12 (**12 mg, 89%, >99% ee). Compounds **10** and **13** were resolved using similar conditions and with excellent separations (α = 1.30 and 1.35, respectively).

Aqueous Solvolysis of *N*-BOC-CPI (13). A sample of **13** (150 μg) was dissolved in CH_3OH (1.5 mL), and the resulting solution was mixed with aqueous buffer (pH 3.0, 1.5 mL, 4:1: 20 (v:v:v) 0.1 M citric acid, 0.2 M Na_2HPO_4, and deionized water, respectively). The UV spectrum of the solution was measured immediately after mixing and then every 2 h for 24 h and every 8 h for 2 weeks. The total reaction time reflects that required to observe no further change in the spectrum. The decrease in absorbance was monitored at 343 nm while the increase was monitored at 238 nm. The solvolysis rate (r^2 = 0.998) was calculated from the plot of $\ln[(A_f - A_i)/(A_f - A)]$ vs time; $k = 7.13 \times 10^{-6}$ s^{-1}, $t_{1/2}$ = 27 h (Figure 8).

Acid-Catalyzed Addition of CH_3OH to *N*-BOC-CPI. A solution of **13** (5.0 mg, 17 μmol, 1.0 equiv) in CH_3OH (1.5 mL) was treated with CF_3SO_3H (0.19 mL, 0.011 M, 2.1 μmol, 0.12 equiv) at 0 °C. The reaction was allowed to warm to 25 °C and after 3 h, was quenched by the addition of $NaHCO_3$ (5 mg), filtered through Celite, and concentrated. PTLC (SiO_2, 20 × 20 cm, 25% EtOAc/hexane) afforded **21** (4.1 mg, 76%) as a clear oil: ^{1}H NMR ($CDCl_3$, 400 MHz) δ 8.37 (d, J = 1.9 Hz, 1H), 7.49 (s, 1H), 7.12 (dd, J = 3.0, 2.7 Hz, 1H), 6.39 (d, J = 2.2 Hz, 1H), 4.03 (m, 2H), 3.88 (m, 1H), 3.81 (d, J = 9.0 Hz, 1H), 3.71 (m, 1H), 3.33 (s, 3H), 1.53 (s, 9H; FABHRMS (NBA/NaI) *m/z* 319.1666 (M^+ + H, $C_{17}H_{22}N_2O_4$ requires 319.1658), and **22** (1.0 mg, 18%) as a clear oil: ^{1}H NMR ($CDCl_3$, 400 MHz) δ 8.43 (s, 1H), 7.49 (s, 1H), 7.11 (dd, J = 3.0, 2.4 Hz, 1H), 6.40 (s, 1H), 3.64 (dd, J = 12.0, 6.9 Hz, 1H), 3.48 (s, 3H), 3.34 (m, 2H), 3.22 (dd, J = 6.9, 12.0 Hz, 1H), 2.81 (dd, J = 6.0, 12.7 Hz, 1H), 1.51 (s, 9H); FABHRMS (NBA/NaI) *m/z* 319.1672 (M^+ + H, $C_{17}H_{22}N_2O_4$ requires 319.1658).

HPLC resolution of the reactions of (±)- and (+)-**13** indicating the reaction regioselectivity (4:1) and the S_N2 addition to provide a single enantiomer of **22** from (+)-**13** is shown in Figure 9.

Addition of HCl to *N*-BOC-CPI. A solution of **13** (5.0 mg, 17 μmol, 1.0 equiv) in THF (0.40 mL) was cooled to −78 °C and treated with 3 M HCl−EtOAc (10.0 μL, 30 μmol, 1.8 equiv). The mixture was stirred for 2 min before the solvent was removed in vacuo. Chromatography (SiO_2, 0.7 × 7 cm, 50% EtOAc/hexane) afforded **12** (5.3 mg, 97%).

General Procedure for the Synthesis of 5-Benzyloxy *seco*-CPI Derivatives. A sample of **10** (1 equiv) was treated with 3.6 M HCl/EtOAc (0.5 mL) at 24 °C for 30 min. The solvent was removed under a stream of N_2, and the residue was dried under vacuum. The salt was dissolved in DMF (0.1 M) and treated sequentially with $NaHCO_3$ (5 equiv), the carboxylic acid (1.2 equiv), 1-(3-(dimethylamino)propyl)-3-ethylcarbodiimide hydrochloride (EDCI, 3 equiv), and the suspension was stirred at 24 °C for 15−18 h under Ar. The

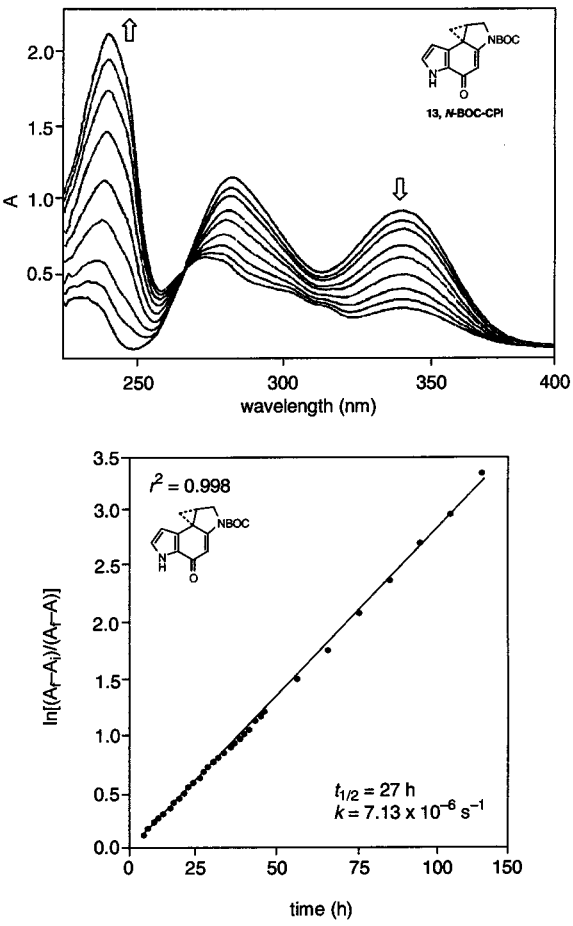

Figure 8. Top: Solvolysis study (UV spectra) of *N*-BOC-CPI (**13**) in 50% CH_3OH−aqueous buffer (pH 3, 4:1:20 (v/v/v) 0.1 M citric acid, 0.2 M NaH_2PO_4, and H_2O, respectively. For clarity, UV traces at only a few time points are shown: $t = 0$, 2, 4, 8, 12, 18, 24, 30, and 36 h. Bottom: Data from solvolysis at 343 nm.

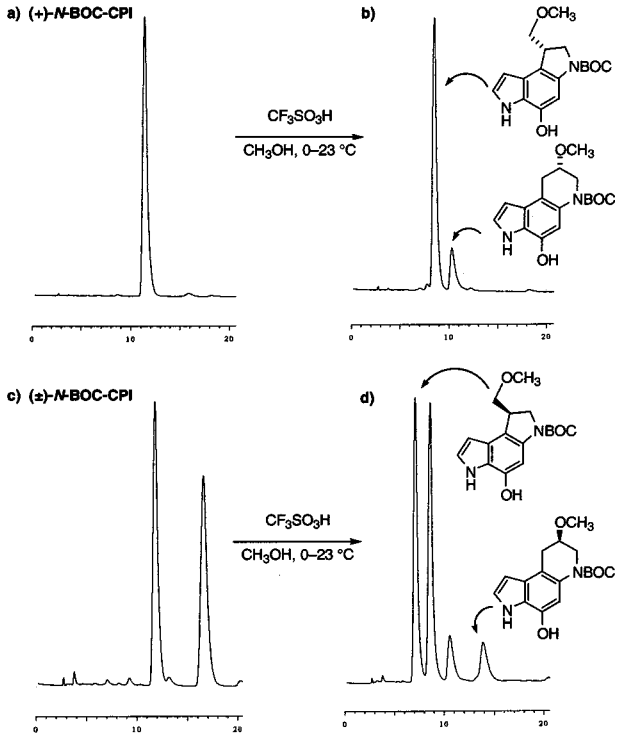

Figure 9. HPLC analysis (Chiracel OD, 10% *i*-PrOH in hexanes) of the acid-catalyzed addition of methanol to *N*-BOC-CPI. (a) (+)-*N*-BOC-CPI. (b) Reaction mixture following acid-catalyzed methanol addition to (+)-*N*-BOC-CPI. (c) (±)-*N*-BOC-CPI. (d) Reaction mixture following acid-catalyzed methanol addition to (±)-*N*-BOC-CPI.

mixture was diluted with H_2O and extracted with EtOAc. The organic layer was dried (Na_2SO_4), filtered, and concentrated in vacuo. Chromatography (40% EtOAc/hexane or 2−4% CH_3OH/CH_2Cl_2) afforded the desired product.[34]

5-(Benzyloxy)-1-(chloromethyl)-1,2-dihydro-3-[(5,6,7-trimethoxy-1*H*-indol-2-yl)carbonyl]-3*H*-pyrrolo[3,2-*e*]indole (28). A sample of **10** (25.0 mg, 0.049 mmol), EDCI (28.1 mg, 0.147 mmol), 5,6,7-trimethoxyindole-2-carboxylic acid (14.7 mg, 0.059 mmol), and $NaHCO_3$ (20.5 mg, 0.244 mmol) in DMF (0.49 mL) afforded **28** (14.8 mg, 56%) as a tan solid: ^{1}H NMR (acetone-d_6, 400 MHz) δ 10.60 (br s, 1H), 10.20 (br s, 1H), 8.06 (br s, 1H), 7.58 (d, J = 7.4 Hz, 2H), 7.33−7.44 (m, 4H), 7.08 (d, J = 2.4 Hz, 1H), 6.99 (s, 1H), 6.60−6.61 (m, 1H), 5.27 (s, 2H), 4.78 (app t, J = 10.4 Hz, 1H), 4.60 (dd, J = 3.7, 10.4 Hz, 1H), 4.13−4.18 (m, 2H), 4.04 (s, 3H), 3.88 (s, 3H), 3.86 (s, 3H), 3.83−3.87 (m, 1H); MALDI−FTMS (DHB) m/z 545.1697 (M^+, $C_{30}H_{28}ClN_3O_5$ requires 545.1717).

(+)-(1*S*)-28: tan solid: $[\alpha]^{23}_D$ +12 (c 7.4 × 10^{-3}, EtOAc).

(−)-(1*R*)-28: tan solid: $[\alpha]^{23}_D$ −14 (c 6.1 × 10^{-3}, EtOAc).

General Procedure for the Synthesis of *seco*-CPI Derivatives. The agents **28**−**32** (1 equiv) in THF (0.07 M) and aqueous HCO_2NH_4 (25%, 22 equiv) were treated with a catalytic amount of 10% Pd/C, and the suspension was stirred at 24 °C for 1 h under Ar. The suspension was filtered (Celite) and concentrated in vacuo. Chromatography (75% EtOAc/hexane or 4% CH_3OH/CH_2Cl_2) afforded the desired product.[34]

(34) Experimental details and full characterization (**29**−**32**, **34**−**37**, and **39**−**42**) are provided in the Supporting Information.

1-(Chloromethyl)-1,2-dihydro-3-[(5,6,7-trimethoxy-1*H*-indol-2-yl)carbonyl]-3*H*-pyrrolo[3,2-*e*]indole (*seco*-CPI-TMI, 33). A sample of **28** (7.4 mg, 0.014 mmol) in 25% aqueous HCO_2NH_4 (0.05 mL) and THF (0.20 mL) afforded **33** (5.8 mg, 94%) as a tan solid: ^{1}H NMR (acetone-d_6, 400 MHz) δ 10.30 (br s, 1H), 10.16 (br s, 1H), 8.72 (s, 1H), 7.83 (br s, 1H), 7.35 (t, J = 2.9 Hz, 1H), 7.06 (d, J = 2.4 Hz, 1H), 6.99 (s, 1H), 6.55 (dd, J = 2.0, 2.9 Hz, 1H), 4.75 (app t, J = 10.4 Hz, 1H), 4.57 (dd, J = 3.7, 10.4 Hz, 1H), 4.08−4.16 (m, 2H), 4.03 (s, 3H), 3.88 (s, 3H), 3.86 (s, 3H), 3.79 (dd, J = 8.5, 10.5 Hz, 1H); FABHRMS (DHB) m/z 455.1248 (M^+, $C_{23}H_{22}ClN_3O_5$ requires 455.1248).

(+)-(1*S*)-33: tan solid: $[\alpha]^{23}_D$ +24 (c 2.8 × 10^{-3}, DMF).

(−)-(1*R*)-33: tan solid: $[\alpha]^{23}_D$ −27 (c 1.2 × 10^{-3}, DMF).

General Procedure for the Synthesis of CPI Analogues. A solution of agents **33**−**37** (1 equiv) in DMF (0.03 M) was treated with NaH (3 equiv, 60% in oil). The suspension was stirred at 24 °C for 30 min, quenched with the addition of phosphate buffer (pH 7), extracted with EtOAc, dried (Na_2SO_4), filtered, and concentrated in vacuo. Chromatography (75% EtOAc/hexane or 4% CH_3OH/CH_2Cl_2) afforded the desired product.[34]

***N*^{2}-[(5,6,7-Trimethoxyindol-2-yl)carbonyl]-1,2,8,8a-tetrahydrocyclopropa[*c*]pyrrolo[3,2-*e*]indol-4-one (CPI-TMI, 38).** A sample of **33** (4.3 mg, 0.010 mmol) and NaH (1.1 mg, 0.028 mmol) in DMF (0.32 mL) afforded **38** (4.0 mg, 100%) as a tan solid: ^{1}H NMR (acetone-d_6, 400 MHz) δ 10.82 (br s, 1H), 10.45 (br s, 1H), 7.14 (t, J = 2.6 Hz, 1H), 7.08 (d, J = 2.4 Hz, 1H), 6.94 (s, 1H), 6.74 (s, 1H), 6.08 (t, J = 2.6 Hz, 1H), 4.53 (dd, J = 5.6, 10.3 Hz, 1H), 4.43 (d, J = 10.3 Hz, 1H), 4.00 (s, 3H), 3.86 (s, 6H), 2.92 (m, 1H), 1.72 (dd, J = 4.3, 8.1 Hz, 1H), 1.57 (t, J = 4.3 Hz, 1H); MALDI−FTMS (DHB) m/z 420.1565 (M^+ + H, $C_{23}H_{21}N_3O_5$ requires 420.1559). This ring closure was also effectively accomplished with DBU in CH_3CN.

(+)-(8a*R*,7b*S*)-38: tan solid: $[\alpha]^{23}_D$ +220 (c 1.7 × 10^{-3}, DMF).

(−)-(8a*S*,7b*R*)-38: tan solid: $[\alpha]^{23}_D$ −220 (c 6.1 × 10^{-4}, DMF).

Acknowledgment. We gratefully acknowledge the financial support of the National Institutes of Health (CA41986) and The Skaggs Institute for Chemical Biology. We thank the Achievement Rewards for College Scientists (ARCS) for a predoctoral fellowship (S.E.W.), the American Cancer Society for a postdoctoral fellowship (S.R.B., 1999−2001), and Dr. Raj K. Chadha for the X-ray structure determination.

Supporting Information Available: Experimental details for the DNA alkylation studies (efficiency, selectivity, and rate), experimental details and full characterization for **29**−**32**, **34**−**37**, and **39**−**42**, a gel figure (Figure S1), and ^{1}H NMR spectra of **5**−**13**, **21**, **22**, and **28**−**42**. This material is available free of charge via the Internet at http://pubs.acs.org.

JO000297J